

# Finite-size-scaling analyses of the chiral order in the Josephson-junction ladder with half a flux quantum per plaquette

Yoshihiro Nishiyama

Department of Physics, Faculty of Science, Okayama University, Okayama 700-8530, Japan

Received: date / Revised version: date

**Abstract.** Chiral order of the Josephson-junction ladder with half a flux quantum per plaquette is studied by means of the exact diagonalization method. We consider an extreme quantum limit where each superconductor grain (order parameter) is represented by  $S = 1/2$  spin. So far, the semi-classical  $S \rightarrow \infty$  case, where each spin reduces to a plane rotator, has been considered extensively. We found that in the case of  $S = 1/2$ , owing to the strong quantum fluctuations, the chiral (vortex lattice) order becomes dissolved except in a region, where attractive intrachain and, to our surprise, repulsive interchain interactions both exist. On the contrary, for considerably wide range of parameters, the superconductor ( $XY$ ) order is kept critical. The present results are regarded as a demonstration of the critical phase accompanying chiral-symmetry breaking predicted for frustrated  $XXZ$  chain field-theoretically.

**PACS.** 75.10.Jm Quantized spin models – 85.25.Cp Josephson devices – 75.40.Mg numerical simulation studies

## 1 Introduction

By means of a field-theoretical technique, Nersesyan, Gogolin and Eßler claimed [1] that the ground state of the  $XXZ$  spin chain with sufficiently strong next-nearest-neighbor interaction is in the chiral phase, where the spin-screw chirality is broken spontaneously. Their proposal is astonishing, because the  $XXX$  counterpart, that has been studied very extensively so far [2,3,4,5,6,7], is known to be in the dimer phase, where the translational symmetry is broken spontaneously so long as the frustration is strong enough. New treatments devised specifically for  $XXZ$  were reported [8,9] so as to support the aforementioned prediction. Meanwhile, as for other frustrated  $XXZ$  chain, namely, the three-leg ladder with diagonal interchain interaction, Azaria *et al.* argued [10,11] that a unique critical phase possessing high central charge ( $c = 2$ ) might be realized in the ground state. According to their argument, the chiral-symmetry breaking is significant to stabilize such high- $c$  criticality. These recent developments tell that the  $XXZ$  anisotropy with in-plane frustration may give rise to unexpected exotic phases. The above-mentioned proposals are all based on field-theoretical descriptions. Therefore, in order to support these scenarios, numerical simulations should be carried out. Kaburagi *et al.* employed the exact diagonalization and the density-matrix renormalization-group methods for the  $XX$  model with the next-nearest-neighbor coupling [12,13]. They concluded that the chirality is *not* broken for the  $S = 1/2$  chain, whereas it would be broken for the  $S = 1$  chain; namely, numerical-simulation result for  $S = 1/2$  appears to contradict the

field-theoretical description. Nevertheless, numerical simulation of such frustrated chain itself is a matter of serious methodological concern [5]; main obstacles are due to the exponentially small energy gap and incommensurability of the spin-correlation function, which often miss-matches the total system sizes.

In order to avoid such complications that would arise from incommensurability, we have investigated the two-leg Josephson-junction ladder,

$$\begin{aligned} \mathcal{H} = & -\frac{t_{\parallel}}{2} \sum_{i=1}^L (e^{i\phi} a_{1i}^\dagger a_{1,i+1} + e^{-i\phi} a_{1,i+1}^\dagger a_{1i}) \\ & -\frac{t_{\parallel}}{2} \sum_{i=1}^L (a_{2i}^\dagger a_{2,i+1} + a_{2,i+1}^\dagger a_{2i}) \\ & -\frac{t_{\perp}}{2} \sum_{i=1}^L (a_{1i}^\dagger a_{2i} + a_{2i}^\dagger a_{1i}) \\ & -V_{\parallel} \sum_{l=1,2} \sum_{i=1}^L a_{li}^\dagger a_{li} a_{l,i+1}^\dagger a_{l,i+1} \\ & -V_{\perp} \sum_{i=1}^L a_{1i}^\dagger a_{1i} a_{2i}^\dagger a_{2i}, \end{aligned} \quad (1)$$

with gauge-twist angle,

$$\phi = \pi. \quad (2)$$

Here,  $a_{li}$  and  $a_{li}^\dagger$  are the hard-core boson annihilation and creation operators, respectively, at the  $i$ -th site along the

$l$ -th leg. The parameters  $t_{\parallel}$ ,  $t_{\perp}$ ,  $V_{\parallel}$  and  $V_{\perp}$  control the intrachain hopping amplitude, the interchain hopping amplitude, the nearest-neighbor intrachain attraction and the interchain attraction, respectively. The number of bosons is set to  $N = L$  (half filled). Throughout this paper, we choose  $t_{\parallel}$  as the unit of energy; namely,

$$t_{\parallel} = 1. \quad (3)$$

We have imposed the periodic-boundary condition along the ladder;  $a_{l,L+1} = a_{l,1}$ . The angle  $\Phi$  denotes the gauge twist around each plaquette. Because the angle is set to  $\Phi = \pi$ , the ladder is subjected to a uniform magnetic field of half a flux quantum per plaquette. That is, suppose that the bosons are in the superconducting state (this is a subtle issue in one dimension), the magnetic flux would possibly be quantized so as to form rigid vortex-lattice order along the ladder. This order is confirmed to develop in the preceding semi-classical analysis [18]. That is, the chiral order of our model has two-unit-cell periodicity. For the purpose of studying the stability of chirality against the quantum fluctuation numerically, our model is far more advantageous than the frustrated spin chain, because the spin-screw chiral order of the latter model has long-wavelength incommensurate structure, and thereby the numerical data suffer from insystematic finite-size-scaling behavior. Tendency to the formation of such vortex structure may become more transparent, if we transform the boson Hamiltonian (1) in terms of spin: Through utilizing the mapping relations between the hard-core boson and the spin-1/2 operators, namely,  $a_{li} = S_{li}^-$ ,  $a_{li}^\dagger = S_{li}^+$  and  $a_{li}^\dagger a_{li} - 1/2 = S_{li}^z$ , the above boson model is mapped to the  $XXZ$  spin ladder,

$$\begin{aligned} \mathcal{H} = & t_{\parallel} \sum_{i=1}^L (S_{1i}^x S_{1,i+1}^x + S_{1i}^y S_{1,i+1}^y) \\ & - t_{\parallel} \sum_{i=1}^L (S_{2i}^x S_{2,i+1}^x + S_{2i}^y S_{2,i+1}^y) \\ & - t_{\perp} \sum_{i=1}^L (S_{1i}^x S_{2i}^x + S_{1i}^y S_{2i}^y) \\ & - V_{\parallel} \sum_{l=1,2} \sum_{i=1}^L S_{li}^z S_{l,i+1}^z - V_{\perp} \sum_{i=1}^L S_{1i}^z S_{2i}^z, \end{aligned} \quad (4)$$

apart from a constant term. Note that the signs of the  $XY$ -component magnetic interactions are different from one leg and the other, and thus an in-plane frustration does exist. Therefore, vortex-antivortex alignment gets favored. The semi-classical version  $S \rightarrow \infty$  of the model (4) has been studied extensively [14,15,16,17,18]: In the limit, spins are represented by rotators, and through path-integral mapping, the system reduces to a two-dimensional classical rotator model. According to numerical-simulation studies [14,15,17], that rotator model appears to be in the KT critical phase. To our surprise, surrounded by such critical background of in-plane spin components, rigid long-range chiral order develops. And so, it is our motivation

to investigate the stability of the chiral order against the quantum fluctuations of  $S = 1/2$ . We show in this paper, that the chiral order fails to develop except in a limited condition, where an attractive intrachain coupling and a repulsive interchain coupling are both turned on. This new phase is a demonstration of critical phase accompanying chiral-symmetry breaking predicted field-theoretically [1,8,9].

Let us mention some remarks concerning the present ladder model described by either boson representation eq. (1) or spin representation eq. (4). One might wonder that the hard-core condition, in other words, the  $S = 1/2$  condition, would be too restrictive, and the model misses microscopic physical ingredients such as the intra-and-inter-grain charge capacitances. Actually, setup of our model might be rather phenomenological. We stress, however, that the one-dimensional  $XXZ$  chains belong to the Tomonaga-Luttinger-liquid universality class irrespective of  $S$  [19]. (Heuristically, it is known that one-dimensional quantum systems possessing the U(1) symmetry are flown to that universality in many cases.) As a matter of fact, according to the proposal [19], the transverse-correlation exponent  $\eta_{\perp}$  is governed by the compact formula,

$$\eta_{\perp} = \frac{\pi - \cos^{-1} J^z}{2\pi S}. \quad (5)$$

(In our notation,  $J^z$  is given by  $J^z = -V_{\parallel}$ .) That is, through varying  $J^z$ , one can cover all possible range of  $\eta_{\perp}$  with  $S = 1/2$  fixed. Lastly, we mention the possibility of the so-called ‘spin liquid’ state that often arises in quantum spin systems; here, the term ‘spin liquid’ denotes the state with exponentially decaying short-range correlation function. we use the term spin liquid that The conventional two-leg ladder [20,21] (with non-frustrated interchain coupling) is a prototypical system exhibiting spin-liquid state. We will show that our frustrated ladder does exhibit spin-liquid phase for a certain parameter condition beside the chiral phase.

This paper is organized as follows. In the next section, we explore the ladder model by means of the exact diagonalization method. The last section is devoted to summary and discussions.

## 2 Numerical results

In this section, we present numerical results. We carried out exact-diagonalization calculations for the system (4) with up to  $N = 2L = 32$  spins. The data are analyzed in terms of the finite-size-scaling theory.

In Fig. 1, we have plotted the Binder parameter [22,23],

$$U = 1 - \frac{\langle M^4 \rangle}{3\langle M^2 \rangle^2}, \quad (6)$$

for the chiral order,

$$M = M_{\text{chiral}} = \sum_{i=1}^L (-1)^i [\mathbf{S}_{1i} \times \mathbf{S}_{2i}]_z$$

$$\begin{aligned}
&= \sum_{i=1}^L (-1)^i (S_{1i}^x S_{2i}^y - S_{1i}^y S_{2i}^x) \\
&= \frac{1}{2i} \sum_{i=1}^L (-1)^i (-a_{1i}^\dagger a_{2i} + a_{1i} a_{2i}^\dagger), \quad (7)
\end{aligned}$$

for the system (1) with  $t_\perp = 0.5$ ,  $V_\parallel = 0.6$  and  $V_\perp$  varied. Here,  $\langle \dots \rangle$  denotes the ground-state average. Note

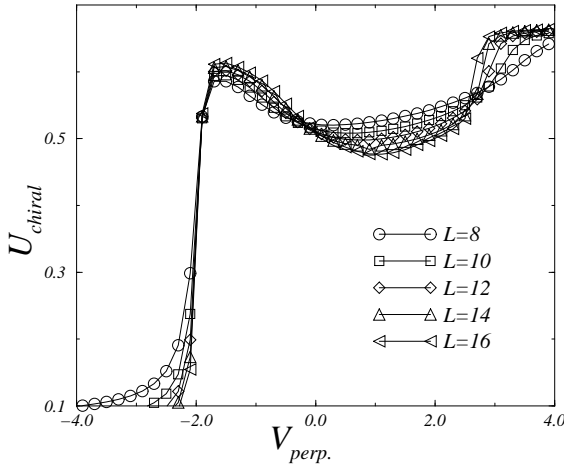


**Fig. 1.** Binder parameter for the chiral order (7) is plotted for  $t_\parallel = 1$ ,  $t_\perp = 0.5$ ,  $V_\parallel = 0.6$  and various  $V_\perp$ . The symbols  $\circ$ ,  $\square$ ,  $\diamond$ ,  $\triangle$  and  $\triangleleft$  denote the data for the system sizes  $L = 8, 10, 12, 14$  and  $16$ , respectively. We see that the chiral order develops in the repulsive interchain coupling  $-1.8 \lesssim V_\perp \lesssim 0$ .

that in the boson language,  $M_{\text{chiral}}$  measures the staggered boson current through the rungs. Therefore, it detects the formation of the vortex-lattice order. Finite-size scaling behavior of the Binder parameter contains the information whether the order  $M$  develops or not [22,23]: If the order is long (short) ranged, the Binder parameter grows (becomes suppressed) through enlarging the system sizes. At critical point, the Binder parameter remains scale-invariant. From Fig. 1, we found that the chiral order develops for the parameter range  $-1.8 \lesssim V_\perp \lesssim 0$ , while it is short ranged otherwise. As would become more apparent in the succeeding analyses, the strong-coupling regions of  $V_\perp \gtrsim 2.5$  and  $V_\perp \lesssim -1.8$  belong to insulator phases of different characters, and are thus rather out of present concern. For  $V_\perp \gtrsim 2.5$ , for instance, the bosons are so cohesive that they may constitute an island in the sea of vacant sites; namely, the system becomes ‘phase separated.’ On the other hand, for  $V_\perp \lesssim -1.8$ , owing to the strong repulsion, a Mott gap opens between the bonding and anti-bonding excitation branches.

Our result shows that the region of the chiral phase is limited. Hence, we found that quantum fluctuations are dominating so that unlike the semi-classical case, assistance of the many-body correlations of  $V_\parallel$  and  $V_\perp$  is vital

for stabilizing the chiral order. After scanning the parameter space, we found that the optimal condition lies around  $t_\perp = 0.5$ ,  $V_\parallel = 0.6$  and  $V_\perp = -1$ . It is fairly reasonable that the optimal intrachain interaction is attractive, because attractive interaction enhances the tendency toward superconductivity ( $XY$  order); see eq. (5), for instance. On the contrary, the fact that the *repulsive* interchain interaction is favorable sounds astonishing. It is expected that the repulsive interchain coupling might enhance the particle exchange between the chains. Hence, we see that such particle exchange is significant in order to confine (pin) the magnetic fluxes at each plaquette.

In order to confirm the above phase diagram, we have calculated the scaled domain-wall energy,

$$L\Delta E(L) = L \left( E_g(L) - \frac{LE_g(L+1)}{L+1} \right). \quad (8)$$

$E_g(L)$  denotes the ground-state energy of the system with

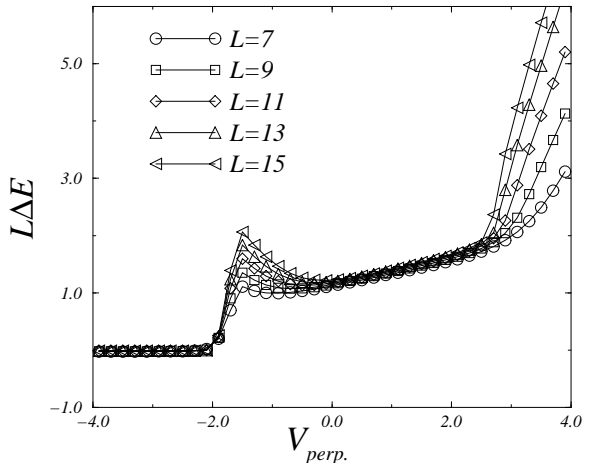


**Fig. 2.** Scaled kink energy (8) is plotted for the same parameter range as that of Fig. 1. The symbols  $\circ$ ,  $\square$ ,  $\diamond$ ,  $\triangle$  and  $\triangleleft$  denote the data for the system sizes  $L = 7, 9, 11, 13$  and  $15$ , respectively. In the region  $-1.8 \lesssim V_\perp \lesssim 0$ , where the chiral phase is realized (see Fig. 1), the scaled kink energy grows actually. On the contrary, in the attractive region  $V_\perp \gtrsim 0$ , the scaled kink energy stays scale-invariant. This indicates that a critical phase, probably of the  $XY$  mode, is realized; see Fig. 3.

size  $L$ , which is supposed to be odd integer. For the system with odd number of plaquettes, one domain wall is created in the alternating alignment of vortex-antivortex structure. As would be apparent from the definition (8),  $\Delta E$  measures the extra domain-wall energy cost due to the kink. Hence, for ordered phase, the scaled kink energy should increase linearly with respect to  $L$ , while for disordered phase,  $L\Delta E$  vanishes exponentially; namely,  $\sim e^{-L/\xi}$  with correlation length  $\xi$ . At critical point,  $L\Delta E$  should be scale-invariant, because  $\Delta E$  is of scaling dimension  $1/L$ ; note the relations  $\Delta E \sim 1/\xi \sim 1/L$ . In Fig. 2,

we plotted  $L\Delta E$  for the same parameter range as that of Fig. 1. In fact, in the chiral phase  $-1.8 \lesssim V_{\perp} \lesssim 0$ , which is estimated from the above Binder-parameter analysis, we observe clear signature of the chiral-domain-wall energy cost. On the other hand, in the area  $0 \lesssim V_{\perp} \lesssim 2.5$ ,  $L\Delta E$  seems to be scale-invariant. In the former analysis of Fig. 1, we have concluded that in the region, the chirality is disordered. Hence, we conclude that in  $0 \lesssim V_{\perp} \lesssim 2.5$ , the  $XY$  order, rather than the chiral order, exhibits criticality. As are mentioned above, the strong-coupling regions of  $V_{\perp} \gtrsim 2.5$  and  $V_{\perp} \lesssim -1.8$  are belonging to insulator phases with different characters. In terms of the pictures presented above, the behaviors of  $L\Delta E$  in these regions are readily understandable. The blowup of  $L\Delta E$  for  $V_{\perp} \gtrsim 2.5$  is due to a kink (dislocation) formed in the island of particles; note that the particle occupation number is forced to be half-filled. On the other hand, the rapid closure of  $L\Delta E$  for  $V_{\perp} \lesssim -1.8$  is precisely due to the fact that the system is a Mott insulator.

Let us turn to the  $XY$  order. In Fig. 3, we plotted the Binder parameter (6) for the in-plane spontaneous magnetization ( $XY$  order), which corresponds to the superconductivity (gauge coherence) order parameter in the boson language,

$$M^2 = M_{XY}^2 = \sum_{limj} (S_{li}^x S_{mj}^x + S_{li}^y S_{mj}^y), \quad (9)$$

for the same parameter range as that of former figures. From the plot, we observe that the  $XY$  order is kept

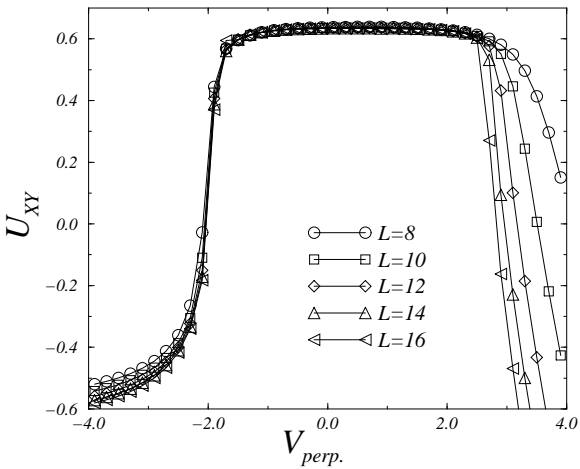


**Fig. 3.** Binder parameter for the  $XY$  order (9) is plotted for  $t_{\parallel} = 1$ ,  $t_{\perp} = 0.5$ ,  $V_{\parallel} = 0.6$  and various  $V_{\perp}$ . The symbols  $\circ$ ,  $\square$ ,  $\diamond$ ,  $\triangle$  and  $\triangleleft$  denote the data for the system sizes  $L = 8, 10, 12, 14$  and  $16$ , respectively. The  $XY$  order appears to be critical in the region  $-1.8 \lesssim V_{\perp} \lesssim 2.5$ . In the region, the fixed point value of the Binder parameter seems to be unchanged. Hence, we see that the  $XY$  order is not influenced by the change of  $V_{\perp}$ .

critical for considerably wide range of parameter  $-1.8 \lesssim$

$V_{\perp} \lesssim 2.5$ . We notice that this  $XY$  critical phase does contain the chiral phase. This feature is quite contrastive to that of the semi-classical case  $S \rightarrow \infty$ , where the chirality is stronger (more stable) than the  $XY$  order, and thus the chiral phase contains the  $XY$  phase [15]. Moreover, it should be noted that in the critical region, the fixed-point value of the Binder parameter is kept hardly changed. In consequence, we found that the  $XY$  correlation function is not influenced very much by  $V_{\perp}$ , while the chiral sector is affected significantly by  $V_{\perp}$ . These results show that those two sectors behave independently; in the commonly referred terminology, those two sectors are ‘separated.’ Such the situation where each mode is described by respective low-energy effective theory occurs commonly in one-dimensional physics. This point is discussed in Section 3.

Lastly, let us turn our attention to the possibility of spin-liquid state. The simplest way to realize the spin-liquid state is given just by setting  $t_{\perp}$  to a very large value. In that strong-interchain-coupling limit, the bonding and anti-bonding excitation branches are separated so that a band gap opens and thereby the ground state becomes disordered. Other than that rather trivial way, we found that the spin-liquid state is accessible from the set of parameters treated in the former figures 1-3 just through setting  $V_{\parallel}$  repulsive; see Fig. 4, where we plotted the Binder parameter for the  $XY$  order for  $t_{\perp} = 0.5$ ,  $V_{\perp} = -1$  and various  $V_{\parallel}$ . We see that for attractive coupling  $0 \lesssim V_{\parallel} \lesssim 0.7$ ,

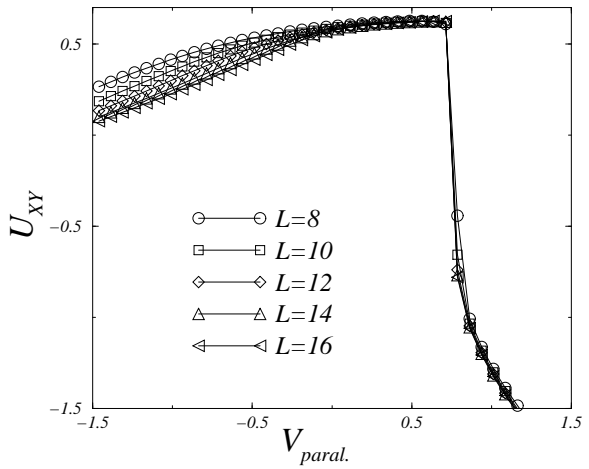


**Fig. 4.** Binder parameter for the  $XY$  order (9) is plotted for  $t_{\parallel} = 1$ ,  $t_{\perp} = 0.5$ ,  $V_{\perp} = -1$  and various  $V_{\parallel}$ . The symbols  $\circ$ ,  $\square$ ,  $\diamond$ ,  $\triangle$  and  $\triangleleft$  denote the data for the system sizes  $L = 8, 10, 12, 14$  and  $16$ , respectively. The  $XY$  order becomes disordered eventually in the repulsive intrachain coupling  $V_{\parallel} \lesssim 0$  and driven to spin-liquid phase.

the  $XY$  sector stays critical as is presented before. (The rapid suppression of  $U_{XY}$  in  $V_{\parallel} \gtrsim 0.7$  is due to phase separation caused by strong attraction.) On the other hand,

for repulsive coupling  $V_{\parallel} \lesssim 0$ , the  $XY$  order becomes disordered eventually and driven to a spin-liquid phase. This behavior tells that the interchain coupling is a relevant perturbation in  $V_{\parallel} \lesssim 0$ . That feature coincides with that of the conventional non-frustrated ladder [24,25,26]. We discuss this similarity in the next section.

### 3 Summary and discussions

We have diagonalized the Josephson-junction ladder subjected to the uniform magnetic field of half a flux quantum per plaquette (1). Unlike the semi-classical case, the chiral order suffers from strong disturbances due to quantum fluctuations. In order to stabilize the chiral order, we need to tune carefully the many-body interactions such as  $V_{\parallel} = 0.6$  and  $V_{\perp} = -1$ . It is surprising that the *repulsive* interchain interaction gives rise to the stabilization of the chiral order. This fact indicates that the particle exchange across the chains over the rungs, rather than the gauge coherence, is vital for pinning the vortices at each plaquette. On the contrary, we found that the  $XY$  order (9) is insensitive to  $V_{\perp}$ ; the  $XY$  order is kept critical for considerably wide range of parameters. This result indicates that the chiral and  $XY$  sectors are separated.

In quantum spin systems, owing to the strong quantum fluctuations, the so-called spin-liquid state can appear [20]. The spin-liquid state, in fact, has been the main concern in the course of studies of the (non-frustrated) two-leg ladder [21]. Close to the chiral phase mentioned above, we found that a spin-liquid state emerges just through changing the sign of  $V_{\parallel}$ . Surprisingly, this behavior coincides with that of the conventional ladder; with the bosonization method [24,25,26], it was shown that the interchain coupling becomes relevant for  $V_{\parallel} \lesssim 0$  (antiferromagnetic intrachain interaction). Hence, it is suggested that the  $XY$  mode of our frustrated ladder and that of the conventional ladder behave similarly. This similarity might be reasonable, if we remember the separation of the chiral and  $XY$  sectors mentioned above. Hence, it is suggested that the present critical phase, as well as that of conventional ladder [24,25,26], belongs to the universality class of the central charge  $c = 1$ . [24,25,26]. Direct identification of the universality class in terms of the finite-size conformal-field theory, for instance, may be exceedingly troublesome, because the excitation structure of the  $XY$  sector is smeared by that of the chiral sector. This would remain for future study.

### Acknowledgments

The author is grateful to Professor I. Harada for helpful discussions.

### References

1. A. A. Nersesyan, A. O. Gogolin and F. H. L. Eßler: Phys. Rev. Lett. **81** (1998) 910.
2. F. D. M. Haldane: Phys. Rev. B **25** (1982) 4925, (E) **26** (1982) 5257.
3. T. Tonegawa and I. Harada: J. Phys. Soc. Jpn. **56** (1987) 2153.
4. I. Harada, T. Kimura and T. Tonegawa: J. Phys. Soc. Jpn. **57** (1988) 2779.
5. S. R. White and I. Affleck: Phys. Rev. B **54** (1996) 9862.
6. D. Allen and D. Sénéchal: Phys. Rev. B **55** (1997) 299.
7. I. Harada and Y. Aoyama: J. Phys. Chem. Solid **60** (1999) 1105.
8. D. C. Cabra, A. Honecker and P. Pujol: Eur. Phys. J. B **13** (2000) 55.
9. D. Allen, F. H. L. Eßler and A. A. Nersesyan: preprint cond-mat/9907303.
10. P. Azaria, P. Lecheminant and A. A. Nersesyan: Phys. Rev. B **58** (1998) 8881.
11. P. Azaria and P. Lecheminant: preprint cond-mat/9912406.
12. M. Kaburagi, H. Kawamura and T. Hikihara: J. Phys. Soc. Jpn. **68** (1999) 3185.
13. T. Hikihara, M. Kaburagi, H. Kawamura and T. Tonegawa: J. Phys. Soc. Jpn. **69** (2000) 259.
14. E. Granato: Phys. Rev. B **45** (1992) 2557.
15. E. Granato: Phys. Rev. B **48** (1993) 7727.
16. C. Denniston and C. Tang: Phys. Rev. Lett. **75** (1995) 3930.
17. E. Granato, J. M. Kosterlitz and M. P. Nightingale: Physica B **222** (1996) 266.
18. J. C. Ciria and C. Giovannella: J. Phys.: Condens. Matter **11** (1999) R361.
19. F. C. Alcaraz and A. Moreo: Phys. Rev. B **46** (1992) 2896.
20. E. Dagotto, J. Riera and D. J. Scalapino: Phys. Rev. B **45** (1992) 5744.
21. E. Dagotto and T. M. Rice: Science **271** (1996) 618.
22. K. Binder: Phys. Rev. Lett. **47** (1981) 693.
23. K. Binder: Z. Phys. B **43** (1981) 119.
24. H. J. Schulz: Phys. Rev. B **34** (1986) 6372.
25. S. P. Strong and A. J. Millis: Phys. Rev. Lett. **69** (1992) 2419.
26. S. P. Strong and A. J. Millis: Phys. Rev. B **50** (1994) 9911.